IEEE Access
Multidisciplinary | Rapid Review | Open Access Journal

Received July 2, 2020, accepted July 12, 2020, date of publication July 16, 2020, date of current version July 28, 2020.

Digital Object Identifier 10.1109/ACCESS.2020.3009676

Development of a Miniature Spectrometer Based on Ultraviolet-Visible Spectroscopy for Quantitative Analysis of Copper and Cobalt

FENGBO ZHOU[1,2], CHANGGENG LI[2], AND ZHU HONGQIU[3]
[1]School of Information Engineering, Shaoyang University, Shaoyang 422000, China
[2]School of Physics and Electronics, Central South University, Changsha 410083, China
[3]School of Automation, Central South University, Changsha 410083, China

Corresponding authors: Fengbo Zhou (fbzhou5018@126.com) and Zhu Hongqiu (hqcsu@csu.edu.cn)

This work was supported in part by the Key Project for International Cooperation and Exchange of the National Natural Science Foundation of China under Grant 61860206014, in part by the State Key Program of National Natural Science of China under Grant 61533021, and in part by the Research Foundation of Hunan Provincial Education Department under Grant 19B518.

ABSTRACT Considering the requirements of miniaturization, integration, digitization and high precision of online detection instrument, a miniature spectrometer based on ultraviolet-visible spectroscopy is developed for the on-line detection of copper and cobalt in the purification process of zinc hydrometallurgy. Firstly, the serial port protocol of spectrometer is developed to realize remote online acquisition of spectral signal. Then, a wavelet threshold denoising method is proposed to eliminate the noise interference caused by the spectrometer and the circuit system. Next, based on the invariance of the dual-wavelength light intensity ratio in the spectral detection, an error correction algorithm is proposed to dynamically eliminate the systematic measurement error caused by light source fluctuations. Finally, the partial least squares method is used to detect the concentration of copper and cobalt, and the detection performance of online miniature spectrometer is compared with that of dual-beam spectrometer. The results show that the developed online analysis instrument can detect polymetal ions in less than 5 min, the average relative error is less than 10%, and the detection accuracy is higher than 94.74%, which is suitable for the online acquisition and analysis of polymetal ions in high concentration zinc solution.

INDEX TERMS Ultraviolet-visible spectroscopy, zinc hydrometallurgy, miniature spectrometer, wavelet threshold method, on-line detection, error correction algorithm.

I. INTRODUCTION

Ultraviolet-visible spectroscopy is a fast analytical method, which has developed rapidly in recent years [1]–[5]. Because of its advantages of many kinds of measurable substances, wide range of measurable concentrations, fast detection speed, good reproducibility, simple instrument and low analysis cost, it is widely used in qualitative and quantitative analysis of substances [6]–[10]. At present, large-scale and precise ultraviolet-visible spectrometers have been widely used in the fields of industry, agriculture, medicine and biology, and are the main analytical equipment in analytical and testing laboratories [11]–[13]. However, these spectrometers use photomultiplier tube devices, which make the detection time long, the equipment huge, the price expensive, and the environment demanding. Therefore, it is only limited to the laboratory and difficult to apply to the industrial site.

With the rapid development of science and technology in the fields of microelectronics, optical technology, optical fiber, computer hardware, and precision instrument manufacturing, the miniature optical fiber spectrometer that integrates the optical splitting and detection functions, has made a breakthrough progress [14]–[17]. At present, there are some mature commercial products, such as Ocean Optical's USB4000, Ideaoptic's PG2000, and optosky's ATP2000, which are widely used in the detection and analysis of ultraviolet spectra, infrared spectra, Raman spectra and other fields [18]–[21]. These miniature spectrometers all adopt new

The associate editor coordinating the review of this manuscript and approving it for publication was Diego Oliva.

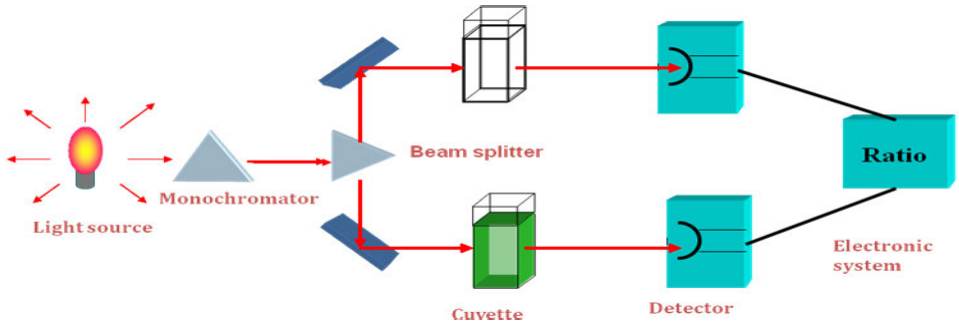

FIGURE 1. Dual beam spectrometer.

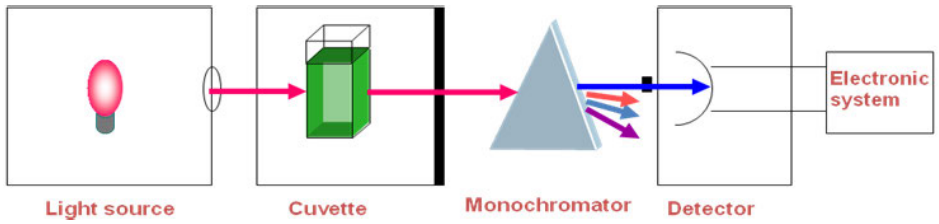

FIGURE 2. Single beam spectrometer.

photoelectric detector, precision optical device and integrated technology, which greatly reduces the volume structure of the instrument, improves the detection resolution and shortens the spectral detection time. The size of the traditional large-scale spectrometer has been shortened by dozens of times, and the price has also been reduced by more than ten times [22]–[25]. Therefore, the miniature spectrometer has the characteristics of miniaturization, integration and fast detection speed, which can be used for on-line detection in the industrial field.

The purification process is a key process of zinc hydrometallurgy, which is the precondition to ensure the normal operation of zinc hydrometallurgy by accurately detecting the concentration of impurity ions in the electrolyte and then removing the impurity ions based on zinc powder replacement method [26]–[30]. At present, the enterprise production still uses manual offline analysis of the concentration of impurity metal ions in the electrolyte. The process is tedious, the detection is time-consuming, and the feedback information is lagging, so it is unable to optimize and adjust the process parameters of the purification process of zinc hydrometallurgy in real time, which leads to the problems of large fluctuation of impurity ion concentration, large consumption of zinc powder and low production efficiency [31]–[33]. Thus, it is very important to realize the online detection and analysis of trace impurity ions in the high-concentration zinc solution. However, the miniature spectrometer is mainly used for on-line detection of multi-component substances with similar concentrations. When detecting impurity ions during the purification process, since the concentration ratio of matrix zinc ion to impurity ions is as high as 10^5, the spectral signal of impurity ions is seriously masked by zinc signal, and it is easy to be interfered by instrument noise and reagent background, resulting in the signal collected by the miniature spectrometer having problems of overflow range and poor accuracy, so it is difficult to detect the concentration of impurity ions online.

The purpose of this paper is to study the online acquisition of spectral signal by a miniature spectrometer, and then propose signal processing algorithms to solve the test errors caused by light source fluctuations, instrument noise, and reagent background interference, and finally use the PLS method for quantitative analysis of impurity metal ions, so as to realize the on-line simultaneous detection of polymetal ions in high concentration zinc solution, and lay the foundation for the efficient and green production of zinc hydrometallurgy.

II. THEORY

A. DETECTION PRINCIPLE

The large spectrophotometer uses a dual-beam structure, as shown in Fig.1. The instrument mainly includes light source, wavelength mechanical scanning structure, monochromator, photomultiplier tube and other components. It has the advantages of ultra-low noise, small stray light, and high test accuracy. However, the disadvantages are large volume and long detection time. Therefore it is mainly used in laboratory off-line analysis. The miniature spectrometer uses a single-beam structure, as shown in Fig.2. The instrument uses a concave flat-field holographic grating full-spectrum beam splitting and a multi-channel array CCD signal receiving technology. Compared with large spectrophotometer, the disadvantage is that the accuracy is lower. However, it has the advantages of small size, fast detection speed, and convenient

carrying, which is suitable for real-time detection in industrial sites.

A single-beam spectrometer can only collect and receive one beam of monochromatic or polychromatic light at the same time, and use two measurements of reference light and measured sample light to perform spectral analysis. The instrument is set to counting mode to detect the intensity of transmitted light, the detection steps are as follows:

(1) Close or obscure the measuring light source, detect the background spectra, and record it as D_λ, where λ represents the wavelength.

(2) Place the reference reagent, turn on the measurement light source, detect the light source spectra, and record it as R_λ.

(3) Place the sample reagent, detect the light source spectra, and record it as S_λ.

If the incident light intensity is I_0, the true transmission light intensity of the reference reagent is I_C, and the true transmission light intensity of the sample reagent is I_P, the following conditions are satisfied:

$$I_C = R_\lambda - D_\lambda \tag{1}$$

$$I_P = S_\lambda - D_\lambda \tag{2}$$

According to Beer-Lambert law, the final absorbance is expressed as:

$$\Delta A = A_P - A_C \tag{3}$$

$$= \lg\frac{I_0}{I_P} - \lg\frac{I_0}{I_C} \tag{4}$$

$$= -\lg\frac{I_P}{I_C} = -\lg\frac{S_\lambda - D_\lambda}{R_\lambda - D_\lambda} \tag{5}$$

Eq. (1)- (5) is the detection principle of the miniature spectrometer. The overall structure diagram of on-line spectral detection of polymetallic ions is shown in Fig. 3.

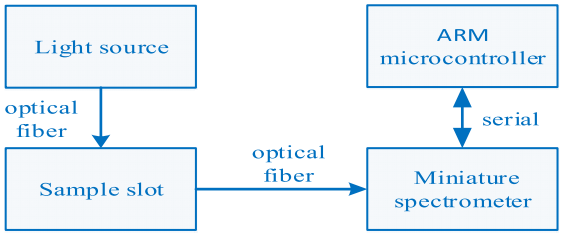

FIGURE 3. The overall structure diagram of on-line spectral detection.

The structure diagram is mainly composed of light source, optical fiber, sample slot, micro spectrometer and ARM microcontroller. The light source is mainly used to provide the band and energy of spectral detection. Optical fiber is used to transmit optical signal and reduce the loss of light in the process of transmission. The sample slot is used to store the substance to be detected. The miniature spectrometer is used to collect spectral signals and convert them into digital signals. The function of ARM microcontroller is to control the parameter setting and process the spectral data, and to interact with the micro spectrometer through serial communication, so as to realize the on-line detection of the spectral signal.

B. WAVELET THRESHOLD DENOISING

The wavelet transform can decompose the signal into an approximation part and a detail part, the approximation part describes the low frequency characteristics of the signal, and the detail part describes the high frequency characteristics of the signal [34]. In the detection of spectral signal, the background interference changes slowly, which is generally concentrated in the low-frequency part of the signal; while the noise changes rapidly, which is concentrated in the high-frequency part of the signal. Therefore, using the multi-resolution of wavelet transform can eliminate background interference and noise. If f(t) represents the original signal, and use wavelet transform to decompose it into J layers. The wavelet transformed signal x(t) satisfies:

$$x(t) = A_J(t) + \sum_{j\le J} D_j(t) \tag{6}$$

In Eq.(6), $A_J(t)$ represents the approximate signal of the J-th layer, $D_j(t)$ represents the detail signal of the j-th layer ($1 \le j \le J$). The approximate signal and the detail signal satisfy the following relationship:

$$A_{J-1}(t) = A_J(t) + D_J(t) \tag{7}$$

Compared with the effective signal, the background interference has a lower frequency and the noise has a higher frequency. Therefore, a threshold denoising method based on wavelet transform is proposed to remove low-frequency background and high-frequency noise of spectral signal. The method includes the following three main aspects: wavelet decomposition, wavelet reconstruction, and peak correction. First, the signal is separated into different frequency components by the discrete wavelet transform, and the background interference concentrated in the low-frequency is removed. Then, inverse wavelet transform is performed to obtain a reconstructed signal. Finally, peak reconstruction is performed on the reconstructed signal to obtain a pure spectral signal. Traditional threshold functions include hard threshold and soft threshold functions. Both of these threshold functions have disadvantages, the hard threshold function is discontinuous at the threshold, while the soft threshold function has a constant deviation between quantized wavelet coefficient and decomposed wavelet coefficient. To overcome the drawbacks of traditional threshold functions, a new threshold function is defined as:

$$\overline{w}_{j,k} = \begin{cases} w_{j,k} - sign(w_{j,k})T(1-\alpha), & |w_{j,k}| \ge T \\ \alpha w_{j,k} 2^{-0.15(|w_{j,k}|-T)^2}, & |w_{j,k}| < T \end{cases} \tag{8}$$

where α is in the range 0 to 1. Since the amplitude of the noise in the spectral signal is random noise obeying Gaussian distribution, the optimal value of α is set to 0.56.

C. SPECTRAL ERROR CORRECTION

Based on the invariance of the dual-wavelength light intensity ratio in the spectral detection, a correction method for the spectral absorbance curve is studied to dynamically eliminate the measurement error of the optical system. For any measured solution's spectral curve, take a wavelength with a smaller absorbance as the reference wavelength to correct the absorption spectral curve. The specific idea is as follows:

$$A_c(\lambda) = A(\lambda) - A(\lambda_R) \tag{9}$$

where, $A(\lambda)$ is the measured absorption spectral curve, $A(\lambda_R)$ is the absorbance value corresponding to the reference wavelength λ_R, and $A_c(\lambda)$ is the corrected spectral curve. Eq. (8) can be expressed in the form of light intensity as follows:

$$A_c(\lambda) = \lg\frac{I_0(\lambda)}{I(\lambda)} - \lg\frac{I_0(\lambda_R)}{I(\lambda_R)} \tag{10}$$

where, $I_0(\lambda)$ and $I_0(\lambda_R)$ are the transmitted intensity of the reference reagent, $I(\lambda)$ and $I(\lambda_R)$ are the transmitted intensity of the sample reagent. Through the mathematical transformation of Eq. (9), we can get:

$$A_c(\lambda) = \lg\frac{I(\lambda_R)}{I(\lambda)} - \lg\frac{I_0(\lambda_R)}{I_0(\lambda)} \tag{11}$$

It can be seen from Eq. (11) that the correction spectral curve $A_c(\lambda)$ is the ratio operation of light intensity signal at different wavelengths. According to the invariant characteristic of the dual-wavelength light intensity ratio in the spectral detection, the correction spectra will not change with the disturbance or drift of the light source signal, thereby dynamically correcting system measurement error caused by the optical detection system. The spectral error correction algorithm is shown in Fig. 4.

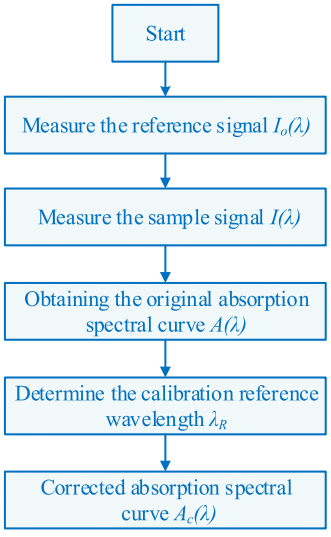

FIGURE 4. Spectral error correction algorithm.

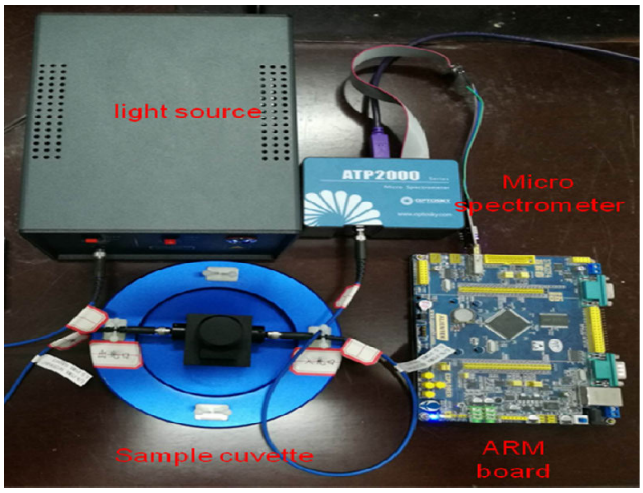

FIGURE 5. The hardware device for online detection of polymetal ions.

III. EXPERIMENTAL

A. EXPERIMENTAL DEVICE

An experimental device is designed for online detection of polymetal ions in high-concentration zinc solution, as shown in Fig. 5. The device mainly consists of light source, optical fiber, cuvette holder, sample slot, micro spectrometer, and ARM microcontroller. Each module of the device has great independence, which is conducive to replacement, maintenance and installation. The light source is a halogen-deuterium mixed light source, which provides spectral energy signals in the ultraviolet-visible band. The quartz cuvette is used to store the test solution and is placed in the sample tank, and the cuvette holder is used to fix the sample tank. An Optosky ATP2000 micro spectrometer (Optosky Technology Ltd., China) is used to measure ultraviolet-visible spectra. The spectrometer can measure the spectral range from 200nm to 1100nm, which meets the detection of spectral energy signal in the ultraviolet-visible band. In addition, the instrument manufacturer provides the serial interface, which is conducive to the realization of the on-line spectral analysis of the polymetallic ions. The ARM microprocessor uses a high-performance processor model STM32F407. The processor adopts the multi-bus matrix AHB (Advanced High-performance Bus), multi-channel DMA (Direct Memory Access), and 168MHz clock frequency, which can effectively improve the program operation efficiency and execution speed.

B. SAMPLES

All reagents were of analytical reagent grade. Deionized water was used for all the dissolution and dilution in the experiment. Using water as a solvent, stock solutions of 50 g/L of zinc (Zn), and 12.5 mg/L of copper (Cu) and cobalt (Co) were prepared by corresponding reagents. Standard solutions were then prepared from the stock standard by serial dilution as required. A series of mixed

standard solutions containing various proportions of zinc and trace ions, 5.00 ml nitroso-R salt solution, 7.5 ml acetic acid-sodium acetate solution were placed in a 25-ml calibrated flask and diluted to the mark with the appropriate volume of distilled water. A blank solution was prepared in the same manner. The final concentration ranges were 0.3–3 mg/L for cobalt, and 0.5–5 mg/L for copper. Absorption spectra were measured by the Optosky ATP2000 spectrophotometer in the wavelength range of 200–1100 nm, with respect to a reagent blank. All the spectra measured were the average of 5 replicates, and they were used for subsequent analysis.

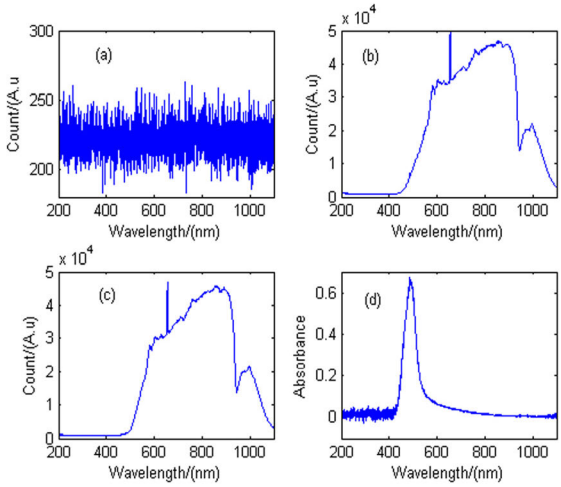

FIGURE 6. Acquisition of spectral signal. (a) The background light intensity. (b) The light intensity of the reference solution. (c) The light intensity of the copper solution. (d) The absorbance spectra of copper.

IV. RESULTS AND DISCUSSION

A. ACQUISITION OF SPECTRAL SIGNAL

Based on the detection principle of the miniature spectrometer, a group of 0.3 mg/L copper solution and a group of reagent blank reference solution were prepared to collect the spectral signal of copper. The ATP2000 spectrometer is designed in a counting mode to collect the intensity of transmitted light. The ARM processor controls the parameter setting of the micro spectrometer through the serial port, and analyzes and processes the spectral data collected by the micro spectrometer to achieve online acquisition of spectral signal. The light intensity of reference solution and copper solution are measured by ATP2000 in the wavelength range of 200-1100nm. as shown in Fig. 6. Fig.6 (a) shows the background light intensity when the light source is turned off. Fig.6 (b) shows the light intensity of the reference solution. Fig.6 (c) shows the light intensity of the copper solution. Obviously, the light intensity of the copper solution is lower than that of the reference solution, because the copper complex in the solution has a strong absorption effect on light, which reduces the transmission intensity of light. According to Eq. (5), the absorbance spectra of copper can be obtained, as shown in Fig.6 (d).

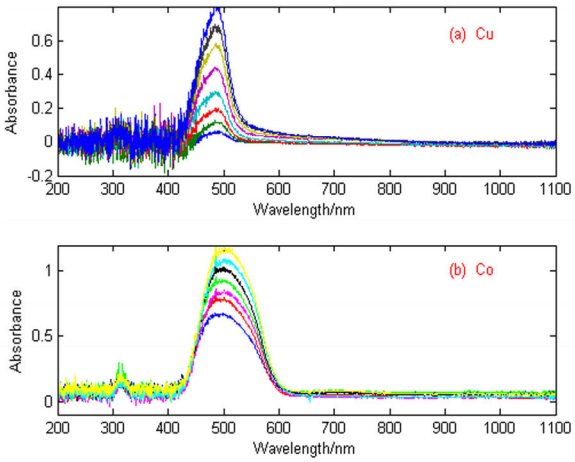

FIGURE 7. Absorbance spectra of Cu and Co in the mixed zinc solution. (a) Cu. (b) Co.

B. SPECTRAL CHARACTERISTICS

Fig.7 shows the ultraviolet-visible absorption spectra of copper (Cu) and cobalt (Co) in high concentration zinc solution at a wavelength range of 200-1100 nm, where the concentration range of copper is 0.5-5.0 mg/L and the concentration range of cobalt is 0.3-3.0 mg/L. We can see from Fig. 7 that the spectral signals of Cu and Co are interfered by noise, especially the copper spectra is more severely affected. The wavelength corresponding to the maximum absorbance of copper and cobalt is 484.66 nm and 503.47 nm respectively. To evaluate the linearity of Cu and Co, The calibration curves of Cu and Co are constructed using the absorbance at their maximum peak and the corresponding concentration, as shown in Fig. 8. As can be seen from Fig.8(a) and Fig.8 (b), the Cu and Co have poor linearity. Their linear equations and correlation coefficients (R^2) are: Abs. = 0.1698 C_{Cu}+ 0.0048 (R^2 = 0.9914) and Abs. = 0.2501 C_{Co}+ 0.5564 (R^2 = 0.9937), respectively. Therefore, it is necessary to preprocess the spectral signal to improve the detection accuracy.

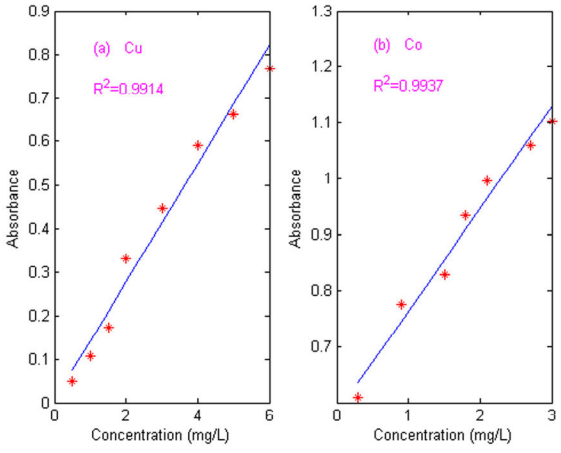

FIGURE 8. Calibration curves of copper and cobalt. (a) Copper calibration curve. (b) Cobalt calibration curve.

C. SPECTRAL PREPROCESSING

The miniature spectrometer has the advantages of modularity, miniaturization, intelligence, and fast detection speed, but compared to large dual-beam spectrophotometer, miniature spectrometer adopts single-beam structure and CCD detector. The single-beam spectrometer can only collect and receive a beam of monochromatic or polychromatic light at the same time, and analyze and detect the spectral signal by measuring the reference light and the sample light separately, which can not offset the noise interference from the external environment (such as temperature, vibration), and the noise interference caused by the spectrometer and the circuit system, resulting in the low photometric accuracy. CCD detector has the advantage of fast detection speed, but the disadvantage is that it enlarges the noise accordingly. Therefore, noise has always been a difficult problem to solve, which directly affects the detection performance of the spectrometer.

Due to the interference of noise on the spectral signal, if the spectral data is modeled directly without denoising pretreatment, it will seriously affect the accuracy of simultaneous detection of copper and cobalt. A threshold denoising algorithm based on wavelet transform is proposed to preprocess the spectral signal to eliminate low-frequency background and high-frequency noise. Fig. 9(a) and Fig. 9(b) show the denoising signals for Cu and Co by the threshold denoising algorithm, respectively. It can be seen from Fig.9 that the noise is completely eliminated, the Cu and Co signals after denoising are smooth, and the spectral shape is consistent with the expected.

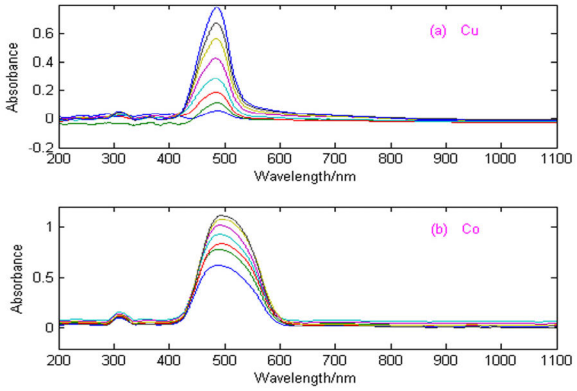

FIGURE 9. The denoising signals for Cu and Co by the proposed threshold denoising method. (a) The denoising signal for Cu. (b) The denoising signal for Co.

In order to evaluate the performance of the threshold denoising algorithm, the original spectral signal of Cu and Co and the spectral signal after pretreatment are linearly corrected under different wavelengths, and the statistical results of the linear correlation coefficient are shown in Table 1. It can be seen that the linear correlation coefficients of Cu and Co at different wavelengths after signal processing have been significantly improved, and the maximum correlation coefficients of Cu and Co are 0.9946 and 0.9958, respectively.

TABLE 1. Statistical results of Cu and Co before and after pretreatment.

Wavelength/nm	Experimental spectral signal		Preprocessed spectral signal	
	Cu	Co	Cu	Co
371.65	0.5123	0.6241	0.5515	0.6634
418.52	0.5708	0.8667	0.6844	0.9227
452.76	0.5004	0.5815	0.7002	0.6943
492.43	0.9813	0.9765	0.9946	0.9922
518.25	0.9736	0.9788	0.9933	0.9958
545.31	0.9831	0.9866	0.9924	0.9937

The results show that the linearity of copper and cobalt has been significantly improved. Therefore, the proposed wavelet threshold denoising method can be used to preprocess spectral data before modeling, and improve the accuracy of quantitative analysis of copper and cobalt.

D. SYSTEMATIC ERROR CORRECTION

Due to the spectrometer data shift caused by light source disturbance, there is a large measurement system error in the spectrometer detection system, and the results of repeated detection of the same sample are inconsistent, which affects the repeatability and accuracy of the detection results. In order to solve this problem, this paper carried out a systematic experimental study and found that under the condition that the light source works stably (generally the light source output is stable after half an hour of warm-up), the dual-wavelength intensity ratio of the spectral signal has the characteristic of not changing with time. Therefore, based on this characteristic, the measurement error of the optical system can be eliminated dynamically by correcting the detected absorption spectra, thereby effectively improving the detection accuracy.

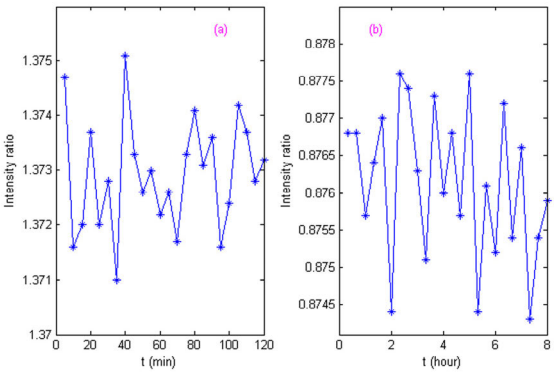

FIGURE 10. The ratio curve of dual wavelength intensity. (a) Ratio curve at the wavelengths of 445nm and 525nm. (b) Ratio curve at the wavelengths of 456nm and 492nm.

In order to test the ratio stability of the light source, iDH2000-BSC light source was used to continuously measure and record with 0.3mg/L copper solution as the test object. Fig. 10 (a) shows the ratio curve of the light intensity with time at the wavelengths of 445nm and 525nm. The test is continued for 2 hours after the light source is turned on

TABLE 2. The predicted concentrations of Cu and Co in high concentration zinc solution.

No.	Actual value (mg /L)		Predicted value (mg/L)		RD(%)	
	Cu	Co	Cu	Co	Cu	Co
1	1.50	0.60	1.416	0.632	5.60	5.33
2	3.00	1.20	2.864	1.271	4.53	5.91
3	4.50	1.80	4.733	1.739	5.17	3.38
4	0.50	2.40	0.531	2.343	6.20	2.37
5	2.00	3.00	1.903	3.119	4.85	3.96
6	3.50	0.30	3.377	0.317	3.51	5.67
7	5.00	0.90	5.306	0.941	6.12	4.55
8	1.00	1.50	0.942	1.569	5.81	4.60
9	2.50	2.10	2.656	2.195	6.24	4.52
10	4.00	2.70	4.245	2.638	6.12	2.29
The average relative deviation (%)					5.42	4.26
RMSEP					0.1693	0.0684

and stable, and the measurement and recording are performed every 5 minutes. It can be seen that the fluctuation range of the light intensity ratio is between 1.3710 and 1.3751, and the maximum relative fluctuation range is 0.29%. Fig. 10 (b) is the ratio curve of the light intensity with time at the wavelengths of 456nm and 492nm. The test is continued for 8 hours after the light source is stabilized, and the measurement and recording are performed every 20 minutes. As can be seen that the fluctuation range of the light intensity ratio is between 0.8743 and 0.8776, and the maximum relative fluctuation range is 0.38%. Obviously, this fluctuation range is approximately constant in engineering. Therefore, it can be concluded that the light intensity ratio at any two wavelengths does not change with time at different test moments after the light source is turned on stably.

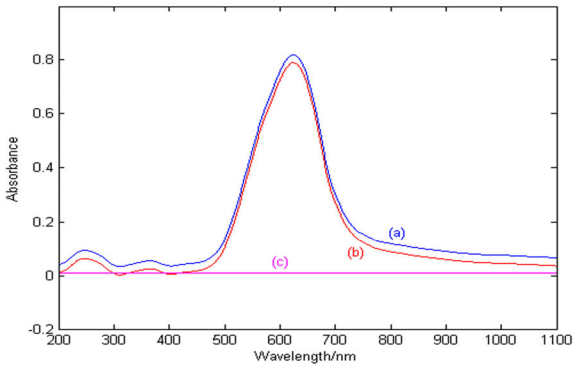

FIGURE 11. Spectral signal correction curve. (a) The original spectral curve. (b) The spectral correction curve. (c) The spectral reference baseline.

The proposed spectral signal correction method is used to process the original spectral signal of copper. The spectral signals before and after correction are shown in Fig. 11. Fig. 11 (a) is the original spectral curve, Fig. 11 (b) is the spectral correction curve, and Fig. 11 (c) is the spectral reference baseline. It can be seen that the corrected spectral shape is more standardized and more repeatable, which is beneficial to eliminate system errors and improve detection accuracy.

E. ONLINE DETECTION OF COPPER AND COBALT

In order to evaluate the performance of the developed online spectrometer, we prepared 10 groups of metal mixed solutions containing Cu and Co in different proportions, and used a 20 g/L zinc solution as a reference. The spectral signal was sampled by ATP2000 spectrometer, and then processed by optical system error correction, noise signal elimination and background interference removal to obtain high-quality signal. The partial least squares method (PLS) were used to detect the concentration of Cu and Co simultaneously in high concentration zinc solution. The predicted concentrations are shown in Table 2, and the prediction accuracy curves are shown in Fig. 12.

As can be seen from Table 2, the maximum relative errors (RD) of Cu and Co are 6.24% and 5.91%, and the average relative errors are 5.42% and 4.26%. the root mean squared error of prediction (RMSEP) is 0.1693 for copper and 0.0684 for cobalt. The predicted and actual values of Cu and Co are shown in Fig. 12(a) and Fig. 12(b). The prediction relative errors of Cu and Co are shown in Fig. 12(c) and Fig. 12(d). It can be seen from Fig. 12 that the predicted values and the actual values of Cu and Co are basically the same, the correlation coefficient (R^2) is 0.9962 for copper and 0.9976 for cobalt, and the relative errors of Cu and Co at different concentrations has small fluctuations. The obtained results display that the developed on-line spectrometer has good detection performance. In order to further compare the performance of the developed on-line spectrometer and experimental dual-beam spectrometer, ATP2000 and dual-beam spectrometer UV-2600 (Shimadzu, Japan)) are used to perform 30 repeatability tests on the experimental data, and the test results are shown in Table 3.

It can be seen from Table 3 that the detection accuracy of the on-line spectrometer is lower than that of the

TABLE 3. Performance comparison of ATP2000 and UV-2600 spectrometers.

Evaluation index	On-line spectrometer ATP2000		Dual-beam spectrometer UV-2600	
	Cu	Co	Cu	Co
Maximum relative error	7.24%	6.31%	6.82%	5.76%
Mean relative error	5.26%	4.32%	4.21%	3.16%
RMSECV	0.204	0.086	0.154	0.063
RMSEP	0.169	0.068	0.097	0.049
Correlation coefficient (R^2)	0.9954	0.9967	0.9971	0.9985
Detection accuracy	94.74%	95.68%	95.79%	96.84%

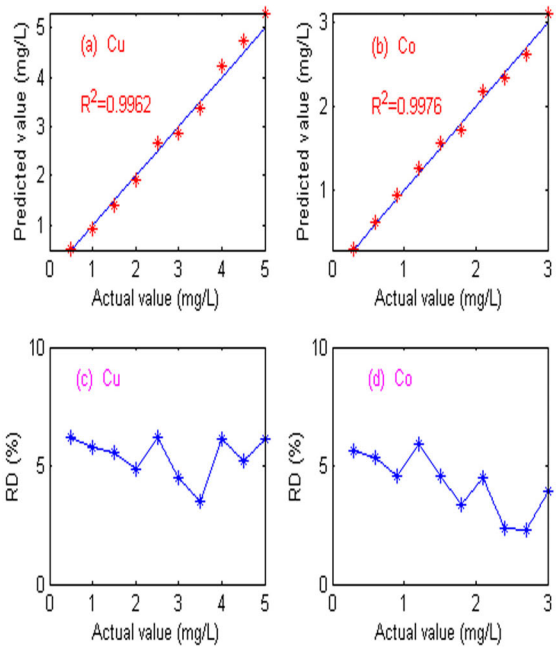

FIGURE 12. Prediction accuracy curves of Cu and Co. (a) Predicted and actual values of Cu. (b) Predicted and actual values of Co. (c) Prediction relative error of Cu. (d) Prediction relative error of Co.

experimental spectrometer, but the detection speed of the on-line spectrometer is fast, the detection time is less than 5 min, the maximum relative errors of Cu and Co are less than 10%, and the detection accuracy of Cu and Co are higher than 94.74%, which meets the requirements of industrial production indexes. The obtained results show that the developed on-line spectrometer is suitable for simultaneous detection of Cu and Co in high concentration zinc solution.

V. CONCLUSION

The large and precise dual-beam UV-visible spectrophotometers is only limited in the laboratory. In the process of industrial production, the samples need to be analyzed off-line in the artificial laboratory. The detection cycle is long and the real-time adjustment is blind, which seriously affects the product quality and production efficiency. The miniature spectrometer can be used for the online detection of metal ion in the industrial field because of its miniaturization, integration, and fast detection speed. However, the miniature spectrometer uses a single-beam structure and a CCD detector, due to the influence of light source fluctuation, instrument circuit noise, reagent background interference and other factors, the measured spectral signal has the problem of overflow range and poor accuracy. In this paper, an on-line detection instrument for the spectral signal of polymetallic ions is designed, and some signal processing algorithms are used to solve the test errors caused by light source fluctuation, instrument noise and reagent background interference to meet the needs of online simultaneous detection of polymetallic ions. The results show that the developed on-line analysis instrument can meet the on-line acquisition and simultaneous detection of polymetal ions in high concentration zinc solution.

REFERENCES

[1] M. Sikder, J. R. Lead, G. T. Chandler, and M. Baalousha, "A rapid approach for measuring silver nanoparticle concentration and dissolution in seawater by UV–Vis," *Sci. Total Environ.*, vol. 618, pp. 597–607, Mar. 2018.

[2] C. Schilling and C. Hess, "CO oxidation on ceria supported gold catalysts studied by combined operando raman/UV–Vis and IR spectroscopy," *Topics Catal.*, vol. 60, no. 2, pp. 131–140, Feb. 2016.

[3] A. Mashkuri, A. Saljooqi, and Z. Tohidiyan, "Nano clay Ni/NiO nanocomposite new sorbent for separation and preconcentration dibenzothiophene from crude prior to UV–vis spectrophotometery determination," *Anal. Chem. Res.*, vol. 12, pp. 47–51, Jun. 2017.

[4] A. R. Martins, M. Talhavini, M. L. Vieira, J. J. Zacca, and J. W. Braga, "Discrimination of whisky brands and counterfeit identification by UV–Vis spectroscopy and multivariate data analysis," *Food Chem.*, vol. 229, pp. 142–151, Aug. 2017.

[5] W. Mäntele and E. Deniz, "UV–VIS absorption spectroscopy: Lambert-Beer reloaded," *Spectrochim. Acta A, Mol. Biomol. Spectrosc.*, vol. 173, pp. 965–968, Feb. 2017.

[6] A. Lambert, M. Asokan, G. Issac, C. Love, and O. Chyan, "Thin-film UV–vis spectroscopy as a chemically-sensitive monitoring tool for copper etching bath," *J. Ind. Eng. Chem.*, vol. 51, pp. 44–48, Jul. 2017.

[7] R. M. Kakhki, M. Nejati-Yazdinejad, and F. Kakeh, "Extraction and determination of Rose Bengal in water samples by dispersive liquid–liquid microextraction coupled to UV–Vis spectrophotometry," *Arabian J. Chem.*, vol. 10, pp. S2518–S2522, May 2017.

[8] K. J. Hamam and M. I. Alomari, "A study of the optical band gap of zinc phthalocyanine nanoparticles using UV–Vis spectroscopy and DFT function," *Appl. Nanosci.*, vol. 7, no. 5, pp. 261–268, Jun. 2017.

[9] V. S. Fedenko, S. A. Shemet, and M. Landi, "UV–vis spectroscopy and colorimetric models for detecting anthocyanin-metal complexes in plants: An overview of in vitro and *in vivo* techniques," *J. Plant Physiol.*, vol. 212, pp. 13–28, May 2017.

[10] A. Dankowska, A. Domagała, and W. Kowalewski, "Quantification of Coffea Arabica and Coffea canephora var. robusta concentration in blends by means of synchronous fluorescence and UV-Vis spectroscopies," *Talanta*, vol. 172, pp. 215–220, Sep. 2017.

[11] E. D. Young, D. Rumble, P. Freedman, and M. Mills, "A large-radius high-mass-resolution multiple-collector isotope ratio mass spectrometer for analysis of rare isotopologues of O_2, N_2, CH_4 and other gases," *Int. J. Mass Spectrometry*, vol. 401, pp. 1–10, Apr. 2016.
[12] X. Si, L. Hu, W. Xu, H. Li, and C. Li, "A dual-source miniature mass spectrometer with improved sensitivity," *Int. J. Mass Spectrometry*, vol. 423, pp. 15–19, Dec. 2017.
[13] H. Shim, J.-W. Lee, B. Hong, J. K. Ahn, G. Bak, J. Jo, M. Kim, Y. J. Kim, Y. J. Kim, H. Lee, H. S. Lee, K. S. Lee, B. Mulilo, D. H. Moon, and M. S. Ryu, "Performance of prototype neutron detectors for large acceptance multi-purpose spectrometer at RAON," *Nucl. Instrum. Methods Phys. Res. A, Accel. Spectrom. Detect. Assoc. Equip.*, vol. 927, pp. 280–286, May 2019.
[14] T. Nakamura and Y. Kondo, "Large acceptance spectrometers for invariant mass spectroscopy of exotic nuclei and future developments," *Nucl. Instrum. Methods Phys. Res. B, Beam Interact. Mater. At.*, vol. 376, pp. 156–161, Jun. 2016.
[15] O. Geiss, C. Cascio, D. Gilliland, F. Franchini, and J. Barrero-Moreno, "Size and mass determination of silver nanoparticles in an aqueous matrix using asymmetric flow field flow fractionation coupled to inductively coupled plasma mass spectrometer and ultraviolet–visible detectors," *J. Chromatography A*, vol. 1321, pp. 100–108, Dec. 2013.
[16] D. Bortot, A. Pola, S. Agosteo, S. Pasquato, M. V. Introini, P. Colautti, and V. Conte, "A miniaturized alpha spectrometer for the calibration of an avalanche-confinement TEPC," *Radiat. Meas.*, vol. 106, pp. 531–537, Nov. 2017.
[17] L. Feng, L. Wei, Y. Nie, M. Huang, L. Yang, X. Fu, and J. Zhou, "Design of a compact spectrometer with large field of view based on freeform surface," *Opt. Commun.*, vol. 444, pp. 81–86, Aug. 2019.
[18] Q. Guo, L. Gao, Y. Zhai, and W. Xu, "Recent developments of miniature ion trap mass spectrometers," *Chin. Chem. Lett.*, vol. 29, no. 11, pp. 1578–1584, Nov. 2018.
[19] B. Lei, J. Wang, J. Li, J. Tang, Y. Wang, W. Zhao, and Y. Duan, "Signal enhancement of laser-induced breakdown spectroscopy on non-flat samples by single beam splitting," *Opt. Express*, vol. 27, no. 15, pp. 20541–20557, Jul. 2019.
[20] C. Markovski, J. M. Byrne, E. Lalla, A. D. Lozano-Gorrín, G. Klingelhöfer, F. Rull, A. Kappler, T. Hoffmann, and C. Schröder, "Abiotic versus biotic iron mineral transformation studied by a miniaturized backscattering Mössbauer spectrometer (MIMOS II), X-ray diffraction and Raman spectroscopy," *Icarus*, vol. 296, pp. 49–58, Nov. 2017.
[21] Z. Ren, M. Guo, Y. Cheng, Y. Wang, W. Sun, H. Zhang, M. Dong, and G. Li, "A review of the development and application of space miniature mass spectrometers," *Vacuum*, vol. 155, pp. 108–117, Sep. 2018.
[22] D. T. Snyder, C. J. Pulliam, and R. G. Cooks, "Extending the mass range of a miniature ion trap mass spectrometer using the inverse mathieu q scan," *Int. J. Mass Spectrometry*, vol. 422, pp. 154–161, Nov. 2017.
[23] Z. Xue, Y. Chen, M. He, X. Xiong, X. Fang, Y. Zhao, and W. Xu, "Development of a miniature mass spectrometer with in-source desolvation," *Int. J. Mass Spectrometry*, vols. 397–398, pp. 1–5, Mar. 2016.
[24] L. Zhou, J. Jiang, K. Zhao, J. Li, C. Wu, H. Li, D. Tian, and K. Hou, "Radiofrequency field enhanced chemical ionization with vacuum ultraviolet lamp for miniature time-of-flight mass spectrometer," *Chin. Chem. Lett.*, vol. 29, no. 5, pp. 707–710, May 2018.
[25] M. Zahmatkesh, H. Spanjers, and J. B. van Lier, "Fungal treatment of humic-rich industrial wastewater: Application of white rot fungi in remediation of food-processing wastewaterr," *Environ. Technol.*, vol. 38, no. 21, pp. 2752–2762, Dec. 2017.
[26] V. Kočanová, J. Cuhorka, L. Dušek, and P. Mikulášek, "Application of nanofiltration for removal of zinc from industrial wastewater," *Desalination Water Treatment*, vol. 75, pp. 342–347, May 2017.
[27] K. Hayat, S. Menhas, J. Bundschuh, and H. J. Chaudhary, "Microbial biotechnology as an emerging industrial wastewater treatment process for arsenic mitigation: A critical review," *J. Cleaner Prod.*, vol. 151, pp. 427–438, May 2017.
[28] Y.-F. Chen, Z.-X. Li, Z.-W. Zhou, Q.-L. Xia, Y.-Z. Nie, and G.-H. Guo, "Nonlinear gyrotropic motion of skyrmion in a magnetic nanodisk," *J. Magn. Magn. Mater.*, vol. 458, pp. 123–128, Jul. 2018.
[29] M. Tahmassebpour, "A new method for time-series big data effective storage," *IEEE Access*, vol. 5, pp. 10694–10699, 2017.
[30] F. Zhou, C. Li, H. Zhu, and Y. Li, "Determination of trace ions of cobalt and copper by UV–vis spectrometry in purification process of zinc hydrometallurgy," *Optik*, vol. 184, pp. 227–233, Mar. 2019.
[31] D. Yadav and R. Banerjee, "A comparative life cycle energy and carbon emission analysis of the solar carbothermal and hydrometallurgy routes for zinc production," *Appl. Energy*, vol. 229, pp. 577–602, Nov. 2018.
[32] J. Luo, N. Duan, F. Xu, L. Jiang, C. Zhang, and W. Ye, "System-level analysis of the generation and distribution for pb, cu, and ag in the process network of zinc hydrometallurgy: Implications for sustainability," *J. Cleaner Prod.*, vol. 234, pp. 755–766, Oct. 2019.
[33] B. Li, X. Wang, Y. Wei, H. Wang, and M. Barati, "Extraction of copper from copper and cadmium residues of zinc hydrometallurgy by oxidation acid leaching and cyclone electrowinning," *Minerals Eng.*, vol. 128, pp. 247–253, Nov. 2018.
[34] F. Zhou, Y. Li, H. Zhu, C. Zhou, and C. Li, "Signal enhancement algorithm for on-line detection of multi-metal ions based on ultraviolet-visible spectroscopy," *IEEE Access*, vol. 8, pp. 16000–16008, 2020.

FENGBO ZHOU was born in Shaoyang, China, in 1985. He received the B.S. and M.S. degrees from Central South University, Changsha, China, in 2008 and 2011, respectively, where he is currently pursuing the Ph.D. degree. His research interests include process control, artificial intelligence, spectral online detection, intelligent optimization, and automated device research.

CHANGGENG LI was born in China, in 1970. He received the B.S., M.S., and Ph.D. degrees from Central South University, Changsha, China, in 1994, 1999, and 2009, respectively. Since 2009, he has been a Professor with the School of Physics and Electronics, Central South University. He has authored more than 60 articles and holds three patents. His research interests include artificial intelligence, process control, spectral online detection, localization with WSN, Bluetooth, Wi-Fi and heterogeneous networks, and data fusion.

ZHU HONGQIU received the B.S. degree from Dalian Jiaotong University, Liaoning, China, in 1994, and the M.S. and Ph.D. degrees from Central South University, Changsha, China, in 2002 and 2010, respectively. His research interests include the modeling and optimization of complex industrial processes. His awards and honors include the National High Technology Research and Development Program of China Award, the National Natural Science Foundation of China Award, the Natural Science Foundation of Hunan Province Award, and the Chang Jiang Scholars Program Award.